THE
PHYSICAL REVIEW

A journal of experimental and theoretical physics established by E. L. Nichols in 1893

SECOND SERIES, VOL. 166, NO. 3 15 FEBRUARY 1968

Electronic Spectra of Crystalline NaCl and KCl†

D. M. ROESSLER* AND W. C. WALKER
Department of Physics, University of California, Santa Barbara, California
(Received 23 August 1967)

The real (ϵ_1) and imaginary (ϵ_2) parts of the dielectric response function, together with the energy-loss function Im $(1/\hat{\epsilon})$, of freshly cleaved single crystals of NaCl and KCl were obtained in the region 5–28 eV by Kramers-Kronig analysis of near-normal-incidence reflectance spectra. Data were obtained over the entire region at room temperature, and from 5–11 eV at 77°K. The low-temperature spectra of both materials reveal a definite distinction between exciton and interband spectra. Fine structure corresponding to the $n=1$ and $n=2$ members of the $\Gamma_{15}(\frac{3}{2})$ and $\Gamma_{15}(\frac{1}{2})$ exciton series were clearly resolved at 77°K, using a spectral resolution of 2Å. The oscillator strength available for interband transitions has been largely exhausted below 15 eV in both materials, and the reflectance and dielectric response have low magnitudes at higher energies. Plasma-resonance effects occur in both materials, and were identified from the Im$(1/\hat{\epsilon})$ function. The optical data are in good agreement with directly measured electron energy losses. The ϵ_2 spectrum of NaCl bears a strong resemblance to that of MgO, and an attempt was made to analyze the observed structure in terms of a band structure similar to that calculated for MgO. On this basis, nearly all of the main spectral features below 14 eV could be identified in terms of direct interband transitions. Strong transitions producing M_0 edges were assigned to the symmetry points Γ, L, and X. A peak at 11.2 eV results from near degeneracy of the $\Delta_5\rightarrow\Delta_1$ and $\Sigma_4\rightarrow\Sigma_1$ transitions. The band gap for the lowest-energy direct transition ($\Gamma_{15}\rightarrow\Gamma_1$) was estimated to be 8.97±0.07 eV at 77°K. The spectrum of KCl is more complex than that of NaCl, because of the low-lying d-like states in the conduction-band structure. The X_3 level lies below X_1, and the exciton associated with it (excited from X_5') produces the temperature-dependent peak at 9.38±0.03 eV (77°K). The band gap ($\Gamma_{15}\rightarrow\Gamma_1$) lies at 8.69±0.07 eV at 77°K, and the remainder of the analysis is analogous to that for NaCl and MgO.

1. INTRODUCTION

THE recent success of combined studies of electronic spectra and pseudopotential band-structure calculations in deriving the electronic structure of a variety of solids has generated interest in extending the method to ionic materials.[1] In particular, the excellent agreement between experimental spectra and pseudopotential calculations obtained for MgO [2] shows clearly the importance of studying related alkali halides such as NaCl and KCl.

Intrinsic electronic spectra of both NaCl and KCl have been obtained previously by a variety of investigators using several techniques. Recent thin-film transmission measurements on the alkali halides have included work on both materials at 80 [3] and 10°K.[4] The bulk crystals have also been studied in detail recently by means of reflectance techniques,[5,6] and the basic spectral features now appear to be rather well established, at least in the region of the lowest-energy electronic transitions. For maximum usefulness in combination with pseudopotential calculations, however, the main features of the complex dielectric response function $\hat{\epsilon}$ must be known with an energy resolution of about 0.1 eV over as wide an energy range as possible, usually at least up to 10 eV beyond the threshold. Perhaps the most useful technique to date for obtaining such data consists of resolving the near-normal-incidence reflectance spectrum from freshly cleaved crystals into the real and imaginary parts of $\hat{\epsilon}$ by dispersion-relation analysis. In order to reduce the lifetime broadening of important spectral features for materials in which ex-

† Work supported by the National Aeronautics and Space Administration.
* Present address: Bell Telephone Laboratories, Murray Hill, N.J.
[1] M. L. Cohen and T. K. Bergstresser, Phys. Rev. **141**, 789 (1966).
[2] M. L. Cohen, P. J. Lin, D. M. Roessler, and W. C. Walker, Phys. Rev. **155**, 992 (1967).
[3] J. E. Eby, K. J. Teegarden, and D. B. Dutton, Phys. Rev. **116**, 1099 (1959).
[4] K. Teegarden and G. Baldini, Phys. Rev. **155**, 896 (1967).
[5] T. Miyata and T. Tomiki, J. Phys. Soc. Japan **22**, 209 (1967).
[6] T. Tomiki, J. Phys. Soc. Japan **22**, 463 (1967).

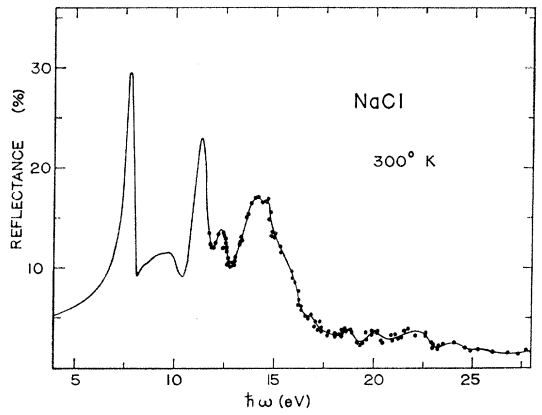

FIG. 1. Reflectance spectrum of freshly cleaved sodium chloride at room temperature. The measurements were made at near-normal incidence (8°).

citons are prominent reflectance spectra at temperatures well below the Debye temperature of the crystal are required.

In the present work, near-normal-incidence reflectance spectra of freshly cleaved NaCl and KCl were obtained at 300°K from 5–28 eV and at 77°K from 5–12 eV. The data were analyzed for $\hat{\epsilon}=\epsilon_1+i\epsilon_2$ by a particular application of the Kramers-Kronig relation which has been described elsewhere.[7]

An important result of this study is a detailed confirmation of the strong similarity between the spectra of MgO and NaCl which had been suggested earlier by Roessler.[8] Because of this similarity an analysis nearly identical to that of MgO was found to explain the NaCl spectrum in some detail. Pseudopotential calculations give essentially this same conclusion.[9]

Although the spectrum of KCl is more complex than that of NaCl the analogy with MgO can still be used to explain many of the features.

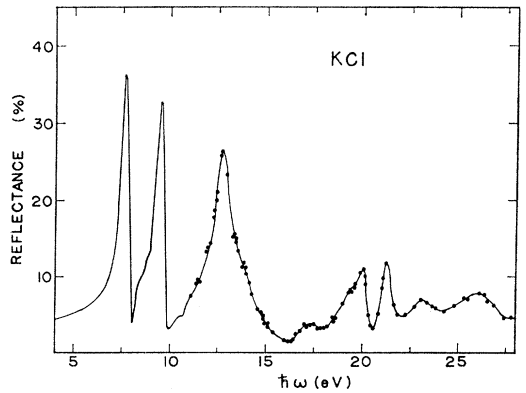

FIG. 2. Reflectance spectrum of freshly cleaved potassium chloride at room temperature.

[7] D. M. Roessler, Brit. J. Appl. Phys. **16**, 1119 (1965); **17**, 1313 (1966).
[8] D. M. Roessler, Ph.D. thesis, University of London, 1966 (unpublished).
[9] C. Y. Fong, W. Saslow, and M. L. Cohen (to be published).

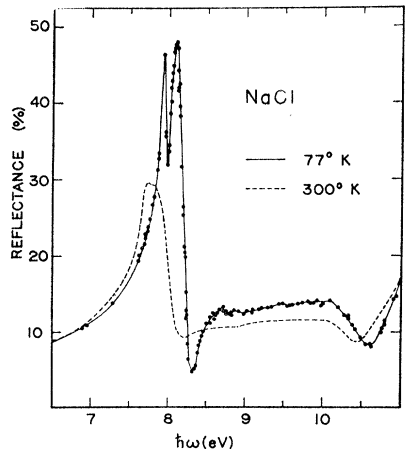

FIG. 3. Temperature dependence of the reflectance spectrum of NaCl below 11 eV.

The additional features of the KCl spectrum were found to derive from a distinct lowering of the *d*-like X_3 state compared to that of NaCl and the introduction of an X point exciton from the resulting X_5'-X_3 edge.

2. EXPERIMENTAL PROCEDURE

Bulk crystals of both materials were obtained from the Harshaw Chemical Co. and, in addition, some of the KCl surfaces examined were prepared from a zone-purified crystal obtained from the Westinghouse Electric Corporation. The use of freshly cleaved surfaces minimizes the likelihood of obtaining reflectance not intrinsic to the material, and the internal evidence from the present data is that surface contamination was negligible.

Ultraviolet radiation at photon energies below 15 eV was provided by a hydrogen discharge, while extension of the measurements to 28 eV was achieved by use of a pulsed high-voltage discharge in argon. Further details of the apparatus have been given elsewhere.[10,11] The experimental measurements of the reflectance are accurate to about 3% below 15 eV, but only to about 10% in some regions beyond 15 eV, as estimated from the scatter of the original data points and the reproducibility of the spectrum. The derived parameters ϵ_1 and ϵ_2 have an additional uncertainty due to the approximation used in the Kramers-Kronig analysis. This has been discussed in detail elsewhere[7] and becomes important only beyond about 26 eV.

In order to maintain the high vacuum necessary to prevent contamination of the samples at 77°K, a lithium fluoride window was used to seal off the reflectrometer from the monochromator system, and this limited the low-temperature measurements to the energy range below 12 eV.

[10] D. M. Roessler and W. C. Walker, Phys. Rev. **159**, 733 (1967).
[11] D. M. Roessler and W. C. Walker, J. Phys. Chem. Solids **28**, 1507 (1967).

During the reflectance measurements on the KCl crystals certain luminescence features were observed at excitation energies near 7 eV, i.e., to the low-energy side of the intrinsic absorption edge. These effects occurred only temporarily, following the cooling of the samples from 300 to 77°K, and could not be detected after the crystals had been at 77°K for more than 10 min. This feature was not investigated in detail, but it is unlikely that its occurrence (possibly due to thermal-strain effects or bromine-impurity centers) should be considered relevant to discussion of the intrinsic spectrum.

3. RESULTS AND DISCUSSION

The room-temperature reflectance spectra for NaCl and KCl are shown in Figs. 1 and 2, respectively. In the region below 14 eV, the solid line refers to the data obtained by means of the hydrogen discharge. Above 14 eV, the solid curve, in both spectra, represents the best fit to data obtained from the argon discharge. In the latter case, the data points are shown by the solid circles and indicate the experimental scatter. In the case of NaCl, the only comparable data beyond 12 eV are the thin-film transmission measurements of Metzger,[12] which extend to 21 eV and are in fair agreement with the present data. Other reflectance measurements[5,13,14] below 12 eV are in good agreement, both in magnitude and position of spectral features, with those shown here. Philipp and Ehrenreich[15] measured the reflectance of KCl as far as 23 eV, and obtained substantially similar features to those shown here. Below 13 eV, the prominent peaks in Fig. 2 also appear strongly in other reflection[6,13,14] and transmission[3,4] data. The temperature dependence of the low-energy spectrum, i.e., below 12 eV, is shown in Figs. 3 and 4

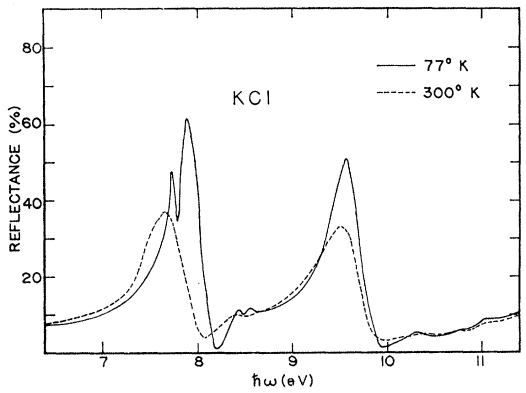

FIG. 4. Temperature dependence of the reflectance spectrum of KCl below 11.5 eV.

[12] P. H. Metzger, J. Phys. Chem. Solids **26**, 1879 (1965).
[13] P. L. Hartman, J. R. Nelson, and J. G. Siegfried, Phys. Rev. **105**, 123 (1957).
[14] J. W. Taylor and P. L. Hartman, Phys. Rev. **113**, 1421 (1959).
[15] H. R. Philipp and H. Ehrenreich, Phys. Rev. **131**, 2016 (1963).

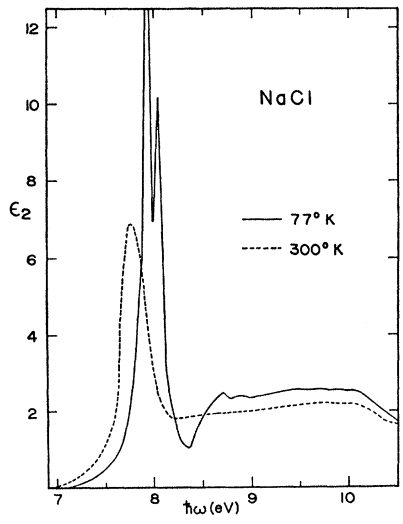

FIG. 5. The ϵ_2 spectrum below 11 eV for NaCl, as derived from a Kramers-Kronig analysis of reflectance data.

where the splitting of the lowest-energy peak is clearly resolved in both crystals.

As emphasized in the preceding section, the reflectance is only of indirect interest, and the Kramers-Kronig relation previously mentioned was used to generate the dielectric parameters ϵ_1 and ϵ_2. In particular, structure in ϵ_2 can be related directly to singularities in the joint density of states for interband transitions.[16] The discussion to follow will therefore be based primarily on the ϵ_2 spectrum. For convenience, the exciton structure nearest the lowest-energy absorption edge will be discussed first.

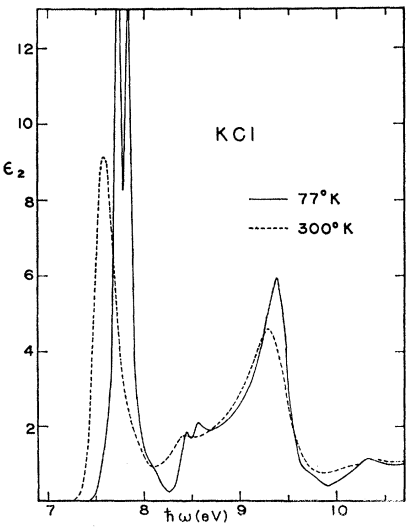

FIG. 6. Temperature dependence of the ϵ_2 spectrum below 11 eV for KCl, as derived from reflectance data.

[16] D. Brust, Phys. Rev. **134**, A1337 (1964).

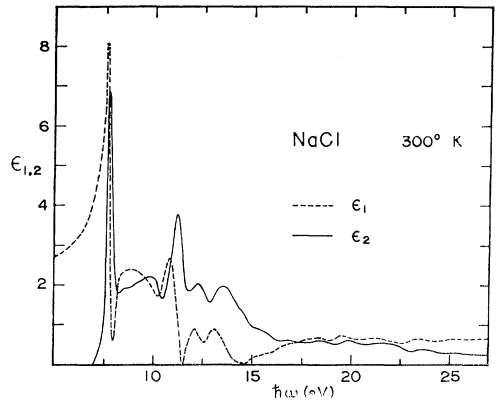

FIG. 7. The dielectric parameters ϵ_1 and ϵ_2 of NaCl. The absolute magnitudes shown for the data beyond 25 eV are uncertain, because of approximations in the computation procedure.

A. Edge Structure

The Coulomb interaction in alkali halides is manifested by the appearance of exciton states in the electronic spectra. Typical of exciton features are the strong temperature dependence and sharpness of the peaks, as compared to interband structure. These characteristics are readily apparent in Figs. 3 and 4, and can also be easily recognized in the derived ϵ_2 spectra shown in Figs. 5 and 6.

Careful studies have recently been made in Japan[5,6] of the reflectance spectra of NaCl and KCl below 12 eV and at temperatures down to 10°K. The resolution of the work permitted a detailed examination of the line shapes and temperature dependence of the excitons, and our discussion of the exciton features will therefore be brief.

The lowest-energy peak in both spectra is due to the creation of an exciton at Γ, the center of the Brillouin zone. The highest valence band in alkali halides is formed primarily from atomic p states of the halide ion, and is spin-orbit split effectively into $j=\frac{3}{2}$, $j=\frac{1}{2}$ levels. In a detailed discussion of this phenomenon, Knox and Inchauspe[17] predicted minimum values for such splittings, including a value of 0.103 eV for alkali chlorides. The room-temperature reflectance data for NaCl exhibit a peak at 7.725±0.025 eV with a shoulder at 7.82±0.03 eV. At 77°K, the spin-orbit splitting produces components at 7.94±0.01 and 8.09±0.01 eV. In ϵ_2 (Fig. 5), the 7.75-eV peak at 300°K is resolved at 77°K into components at 7.92±0.01 and 8.03±0.01 eV. The splitting at 77°K is therefore 0.11±0.02 eV, in good agreement with theory. For KCl, the 7.66-eV reflectance peak (300°K) is split at 77°K into members at 7.75±0.01 and 7.90±0.01 eV. The ϵ_2 spectrum is similar; the 300°K peak at 7.59±0.02 eV gives components at 7.735±0.015 and 7.845±0.015 eV at 77°K. As in NaCl, the spin-orbit splitting is 0.11±0.03 eV, and this therefore corresponds to the valence-band splitting at Γ_{15}. Even though the excitons are tightly bound in alkali halides, there is evidence for a Wannier-like series of exciton lines, and the $n=2$ members of such series can be seen clearly in the reflectance spectra[18] of KI and RbI, for example. In the present work, the $n=2$ states appear only weakly in NaCl (Fig. 3) because of the data scatter; they are more clearly apparent in KCl (Fig. 4). In the ϵ_2 spectra (Figs. 5 and 6) the positions of the $n=2$ states at 77°K are 8.71±0.02 and 8.88±0.02 eV for NaCl, and 8.45±0.02 and 8.57±0.02 eV for KCl. The splittings (0.17±0.04 eV for NaCl and 0.12±0.02 eV for KCl) are consistent with the interpretation given above. Although a purely Wannier-like exciton picture is inappropriate, the appearance of the $n=2$ members permits reasonable estimates of the energies associated with the direct interband edges. On this basis, E_n, the energy of the nth exciton member, is given in terms of the band gap E_G and the exciton binding energy B by the expression

$$E_n=E_G-B/n^2. \quad (1)$$

The exciton associated with the upper ($j=\frac{3}{2}$) of the Γ_{15} valence-band levels has a binding energy of 1.05 eV according to Eq. (1). If we assume the optical value of 1.544 is appropriate for the dielectric constant of NaCl during the exciton transition, then the Γ_{15} ($j=\frac{3}{2}$) exciton has a reduced mass ratio of 0.44 and an effective radius of 2.9 Å (compare the interionic spacing in NaCl, 2.81 Å). For KCl, the corresponding exciton has a binding energy of 0.95 eV, a reduced mass ratio of 0.34, and an effective radius of 3.4 Å (compare the interionic spacing in KCl, 3.14 Å).

Values for the oscillator strengths of the exciton transitions were obtained by a classical dispersion fit to the experimental peaks. This procedure is crude but provides a rough guide to the relative intensities of the $j=\frac{3}{2}$, $\frac{1}{2}$ transitions. For NaCl, the $j=\frac{3}{2}$ member of the Γ exciton doublet has an oscillator strength of about 0.21 per mole, while the $j=\frac{1}{2}$ member is almost as strong (0.19 per mole). The corresponding values for KCl are larger, being 0.31 and 0.38, respectively. For pure j-j coupling the intensity ratio should be 2:1 for the doublet components. The present values (1.1:1 for NaCl and 0.8:1 for KCl) are only approximate but are sufficiently different from 2:1 to indicate that the exchange interaction between the electron and hole is significant. A detailed discussion of the effects of spin-orbit and electron-hole exchange interactions on exciton states in the alkali halides has recently been given by Onodera and Toyozawa.[19]

B. Interband Transitions

As noted in the Introduction, the reflectance spectrum of NaCl (Fig. 1) is remarkably similar to that of

[17] R. S. Knox and N. Inchauspé, Phys. Rev. 116, 1093 (1959).

[18] D. M. Roessler and W. C. Walker, J. Opt. Soc. Am. 57, 677 (1967).

[19] Y. Onodera and Y. Toyozawa, J. Phys. Soc. Japan 22, 833 (1967).

MgO.[2,8,10] Both crystals are face-centered cubic structures, possessing similar Brillouin zones, and this, together with the relative positions of the constituent elements in the periodic table, suggests that the electronic band structures may differ only in minor respects. There have been very few band-structure calculations for NaCl,[20–22] and those of Shockley[20] and Casella[22] were concerned only with the valence bands. The validity of Tibbs's[21] calculation of conduction-band levels has been criticized. Our purpose in the present section is to identify the interband transitions NaCl as far as possible on the assumption of an MgO-like band structure.[9] This treatment will then be further extended to KCl, where the d bands are lower than in NaCl and complicate the conduction-band structure.

The dielectric parameters of NaCl, as computed via a Kramers-Kronig analysis of the reflectance data of Fig. 1, are presented in Fig. 7. Both ϵ_1 and ϵ_2 preserve the spectral features seen in reflectance, but only the ϵ_2 line shapes are directly related to the joint density of states. A schematic diagram of a band structure for NaCl, based upon that of MgO, is shown in Fig. 8. Although the energy scale is arbitrary, the energy gaps which were determined from the present data are drawn approximately to scale. The correct ordering of certain of the conduction-band levels is not known, and the present data are insufficient to determine whether the second conduction-band level at L is in fact L_3' rather than L_1 for example. By analogy with MgO, however, we assume that, at the symmetry points shown, the lowest conduction-band levels are predominantly s-like, and the next conduction-band levels are primarily d-like.

The contribution to ϵ_2, for direct interband transitions where lifetime broadening has been neglected, may be expressed[23] by the relation

$$\epsilon_2(\omega)=\frac{e^2h^2}{m}\sum_{i,j}\frac{1}{\Omega}\int\frac{f_{ij}(\bar{k})}{E_{ij}|\nabla_k E_{ij}|}dS, \tag{2}$$

where

$$f_{ij}(k)=\frac{2}{3m}\frac{|\langle k,i|p|k,j\rangle|^2}{E_{ij}} \tag{3}$$

is the interband oscillator strength, S is a surface of constant interband energy, Ω is the volume of the Brillouin zone, and the interband energy $E_{ij}=E_j-E_i$. For materials such as NaCl, it is not expected that $f_{ij}(k)$ is a strongly varying function, and we therefore assume that the dominant structure in ϵ_2 is determined by the critical points where the integrand in Eq.(2) vanishes. The nature of such critical points, or Van Hove singularities, is now well established,[16,24,25] and we shall adopt the nomenclature in current use, i.e., M_0, M_1, M_2, and M_3 for the principal edge types. Parabolic, or M_0, edges appear in Fig. 7 at about 9.5, 10.5, 11.8, and 12.9 eV, and in the 14–15-eV region and above. The M_0 edges produced by the $\Gamma_{15}\rightarrow\Gamma_1$ transition have already been discussed above with the exciton features, and the energy gaps at 77°K are 8.97±0.07 eV, for the transition to Γ_1 from the upper spin-orbit split Γ_{15} level, and 9.16±0.07 eV for the transition from $\Gamma_{15}(j=\frac{1}{2})$. Spin-orbit splitting of the highest valence band, at points other than Γ, was too small to be observed in the present spectrum and will not be discussed further. As in MgO, we expect the $L_3\rightarrow L_2'$ transition to occur at energies below that required for the first transition at X, i.e., $X_5'\rightarrow X_1$. The strong peak at 11.2 eV in the NaCl spectrum is directly analogous to a similar feature in the MgO spectrum.[2] The latter peak arose from near degeneracies of M_1 and M_2 edges corresponding to transitions at Δ and Σ, respectively, preceded by the strong M_0 edge from the $X_5'\rightarrow X_1$ transition. On this basis we assign a value of 10.5±0.2 eV to the $X_5'\rightarrow X_1$ transition, which produces the strong increase in ϵ_2 beyond the minimum near 10.5 eV. The $\Delta_5\rightarrow\Delta_1$ transition produces an M_1 edge at 11.0±0.2 eV followed by the $\Sigma_4\rightarrow\Sigma_1$, M_2 edge at 11.4±0.2 eV. A value of 9.5±0.3 eV is assigned to $L_3\rightarrow L_2'$, and the M_1 critical point due to the hyperbolic edge at Λ gives a value of 10.0±0.3 eV to the $\Lambda_3\rightarrow\Lambda_1$ transition.

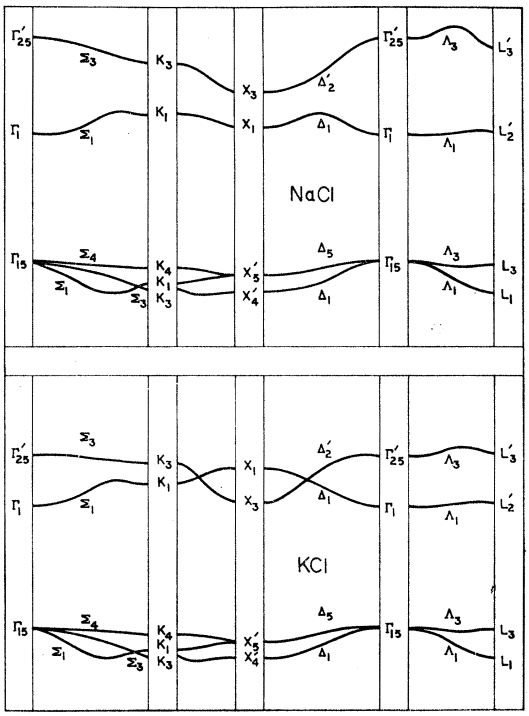

FIG. 8. Schematic band-structure diagrams for NaCl and KCl. The energy levels are only approximately to scale.

[20] W. Shockley, Phys. Rev. **50**, 754 (1936).
[21] S. R. Tibbs, Trans. Faraday Soc. **35**, 1471 (1939).
[22] R. C. Casella, Phys. Rev. **104**, 1260 (1956).
[23] J. C. Phillips, in *Solid State Physics*, edited by F. Seitz and D. Turnbull (Academic Press Inc., New York, 1966), Vol. 18.
[24] L. Van Hove, Phys. Rev. **89**, 1189 (1953).
[25] J. C. Phillips, Phys. Rev. **104**, 1263 (1956).

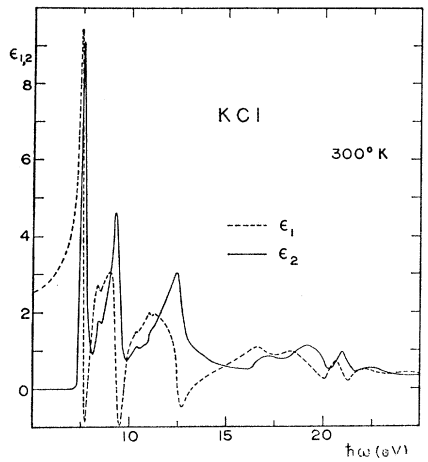

FIG. 9. The dielectric parameters ϵ_1 and ϵ_2 of KCl below 25 eV at 300°K.

It should be noted that excitons are not necessarily confined to Γ, although if the lowest interband transition occurs here, then excitons at X, for example, may be scattered rather easily at the interband threshold and be markedly lifetime broadened. The data of Figs. 3 and 5 do indicate some temperature dependence at X, and if excitons are indeed present (near 10 eV), then the contributions to ϵ_2 predicted by future band-structure calculations should be smaller than observed experimentally in this region. Modulated reflectance studies in the 10-eV region should also resolve spin-orbit-split structure (due to a valence-band splitting of about 0.07 eV at X_5') associated with the exciton; a similar splitting should also appear near 10.5 eV due to the direct interband transition $X_5' \rightarrow X_1$.

By using the MgO analogy we have now identified all the basic features below 12 eV in terms of exciton and interband transitions involving the highest valence band and the lowest conduction band. Interband transitions to the next higher conduction band are more difficult to identify using only the present data.

The increase in ϵ_2 (Fig. 7) beyond the Δ, Σ peak probably arises from transitions at X, by direct analogy with the corresponding feature in MgO. On this basis we give a value of 11.8±0.2 eV to the $X_5' \rightarrow X_3$ transition; the conduction-band separation at X between X_1 and X_3 is therefore 1.3±0.4 eV. The $L_3 \rightarrow L_3'$ transition may be responsible for the strong increase in ϵ_2 at 12.9±0.2 eV. The spectrum beyond 12 eV shows evidence of considerable, but poorly resolved, structure. Identification of critical points is therefore difficult and must await modulated reflectance studies in this region. The strong features remaining are the two structures with peaks near 12.3 and 13.5 eV, respectively. Judging from the weakness of the structure beyond 15 eV, we believe that most of the oscillator strength associated with interband transitions to the lowest two conduction bands has been exhausted below 15 eV. The M_0 edge associated with the $\Gamma_{15} \rightarrow \Gamma_{25}'$ transition should therefore be located in the 12–14-eV region. The increase in ϵ_2 near 12.9 eV, mentioned above, is very strong, and it is possible that $\Gamma_{15} \rightarrow \Gamma_{25}'$ is near degenerate with $L_3 \rightarrow L_3'$. We tentatively assign a value of 13.2±0.3 eV to the $\Gamma_{15} \rightarrow \Gamma_{25}'$ transition. It is doubtful if either of the peaks at 12.3 and 13.5 eV arises from only two or three critical points, although M_1 and M_2 edges probably produce the dominant structure. In the MgO spectrum,[10] a peak occurs at 16.8 eV followed by a second at 17.3 eV. We believe that the transitions responsible for these structures[9] are probably those producing the analogous features in NaCl. Saddle-point edges occur along Δ and Σ; in particular, M_1 edges arise from $\Delta_1 \rightarrow \Delta_1$, $\Delta_5 \rightarrow \Delta_2'$, and $\Sigma_4 \rightarrow \Sigma_1$. Similar edges also occur at $L(L_1 \rightarrow L_2')$ and $X(X_4' \rightarrow X_3)$. The peaks observed are probably due to near degeneracy of these edges with M_2 edges due to transitions along Δ and Σ (for example, $\Sigma_3 \rightarrow \Sigma_1$, $\Sigma_4 \rightarrow \Sigma_2$, and $\Sigma_1 \rightarrow \Sigma_1$). M_3 edges appear to be present just below 13 and 14 eV, respectively; they may be associated with transitions at Δ and $\Lambda(\Lambda_3 \rightarrow \Lambda_3)$. A more detailed investigation necessitates better resolved data and an improved band-structure calculation.

Differences between the KCl and NaCl spectra (Figs. 7 and 9) are more marked than in the case of NaCl and MgO. The most notable dissimilarity is the strong peak at 9.3 eV in the KCl spectrum. This peak is quite temperature-dependent (Figs. 4 and 6) and we believe it is excitonic in origin. There have recently been several band-structure calculations for KCl,[26–28] and a particularly interesting feature of the conduction-band studies[27,28] is that the X_3 level is actually lower than X_1. One might expect X_3 to be lower (relative to X_1) in KCl than NaCl if only because d-like states are more easily accessible in the K^+ ion than in Na^+. The effect is so marked at X, however, that the d-like (X_3) and s-like (X_1) levels are inverted. The usual ordering appears to be preserved at the other main symmetry points in the Brillouin zone, and the schematic diagram given in Fig. 8 reflects the above information. Again we emphasize that the bands shown are drawn only approximately to scale, and are indicated merely for convenience when referring to interband transitions.

We suggest that the peak in the ϵ_2 spectrum at 9.30±0.03 eV is due to an exciton associated with the $X_5' \rightarrow X_3$ transition. At 77°K, the peak moves to 9.38±0.03 eV. There is no clear evidence of spin-orbit splitting in the structure, nor of $n=2$ exciton lines (although these would be very weak in any case); modulated reflectance work should resolve these features. We place the associated M_0 scattering edge ($X_5' \rightarrow X_3$) at 9.9±0.1 eV. The remainder of the spectrum below 10 eV is directly analogous to that of NaCl.

Use of Eq. (1) in the preceding section gives values for the smallest band gap of 8.69±0.07 eV (77°K) for

[26] L. P. Howland, Phys. Rev. **109**, 1927 (1958).
[27] S. Oyama and T. Miyakawa, J. Phys. Soc. Japan **21**, 868 (1966).
[28] P. D. DeCicco, Phys. Rev. **153**, 931 (1967).

the $\Gamma_{15}(\frac{3}{2}) \rightarrow \Gamma_1$ transition and 8.81±0.07 eV for $\Gamma_{15}(\frac{1}{2}) \rightarrow \Gamma_1$. The $L_3 \rightarrow L_2'$ transition gives an M_0 edge at 9.0±0.2 eV, followed by the $\Lambda_3 \rightarrow \Lambda_1$ transition just above 9 eV. The M_1 edge due to the Λ transition is masked by the X exciton structure, but we estimate its position at 9.2±0.2 eV. The feature near 10.4 eV may be due to an M_1 edge, in which case the $\Delta_5 \rightarrow \Delta_1$ transition is a possible interpretation. On the other hand the Δ, Σ transitions produced a very strong peak in NaCl, and the structure near 12.5 eV may be the direct analogy. This assumption would place $\Delta_5 \rightarrow \Delta_1$ at 12.3±0.2 eV, and $\Sigma_4 \rightarrow \Sigma_1$ (giving an M_2 edge) at 12.5±0.2 eV, but we shall discuss objections to this below. The $X_5' \rightarrow X_1$ transition is probably responsible for the increase in ϵ_2 near 11 eV, and we assign to it a value of 10.9±0.3 eV. It is possible that because of the inversion of the X_1, X_3 levels, the $\Delta_5 \rightarrow \Delta_2'$ transition may occur at lower energies than $\Delta_5 \rightarrow \Delta_1'$ and produce an M_1 edge at 10.3±0.2 eV. The parabolic (M_0) edges produced by the $\Gamma_{15} \rightarrow \Gamma_{25'}$ and $L_3 \rightarrow L_3'$ transitions are not clearly resolved, but must account for part of the very strong increase in ϵ_2 in the 11–12-eV region. We tentatively suggest values of 11.2±0.4 eV ($L_3 \rightarrow L_3'$) and 11.6±0.5 eV ($\Gamma_{15} \rightarrow \Gamma_{25}'$) for these transitions. Note, however, that if $\Gamma_{15} \rightarrow \Gamma_{25}'$ lies below 12 eV as suggested, then the M_1 edge at 12.3±0.2 eV can no longer be regarded satisfactorily as due to the previously mentioned Δ transition ($\Delta_5 \rightarrow \Delta_1$). The latter would more probably lie near 11.1±0.2 eV. Similarly, $\Sigma_4 \rightarrow \Sigma_1$ more probably lies near 10.5 eV, the M_2 edge being obscured by neighboring transitions.

The very strong falloff in ϵ_2 beyond 12.5 eV, and extending several electron volts, indicates that most of the oscillator strength available for transitions to the lowest two conduction bands is exhausted, i.e., the prominent transitions occur at energies below 13 eV. The effect of the low-lying d band in KCl is therefore not only to invert the X_1 and X_3 levels, but to cluster critical points in a smaller energy region than in NaCl. The transitions which produced the three strong features in the 10.5–14-eV region of the NaCl spectrum (Fig. 7) are sufficiently close in energy in KCl to produce the single broad hump peaking at 12.4 eV. The present data do not permit a more detailed analysis at this stage, but it is possible that the increase in ϵ_2 beyond 16 eV marks the onset of transitions from the valence band to the third conduction-band levels, such as $\Gamma_{15} \rightarrow \Gamma_{12}$ and $X_5' \rightarrow X_2$.

C. Plasma Effects

There have recently been several studies of the energy losses suffered by electron beams scattered from both NaCl[29–34] and KCl.[29–34] Such work has included studies on both thin films and bulk crystals. The energy distribution of the scattered electrons is determined primarily by the function $\mathrm{Im}(1/\hat{\epsilon})$, where $\hat{\epsilon}$ is the dielectric constant of the material and refers to the longitudinal electron-electron interaction. The transverse dielectric response, for photon-electron interactions, can be shown to be very similar, within the random-phase approximation and in the long-wavelength limit.[35] We therefore expect similarities between the $\mathrm{Im}(1/\hat{\epsilon})$ function computed from the optical data and the directly measured electron energy-loss spectra.

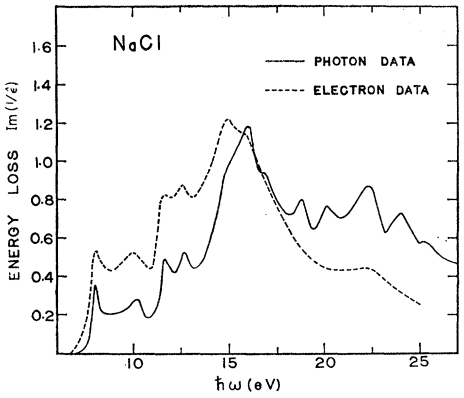

FIG. 10. The energy-loss function $\mathrm{Im}(1/\hat{\epsilon})$ for NaCl, derived from a dispersion analysis of the optical-reflectance data of Fig. 1.

We have computed $\mathrm{Im}(1/\hat{\epsilon})$ for both materials and present the spectra in Figs. 10 and 11. For comparison, we also show, by means of the broken curves, the characteristic electron energy-loss spectra measured directly by Creuzburg.[29] The resemblance between the NaCl spectra is remarkable, not only in the one-to-one cor-

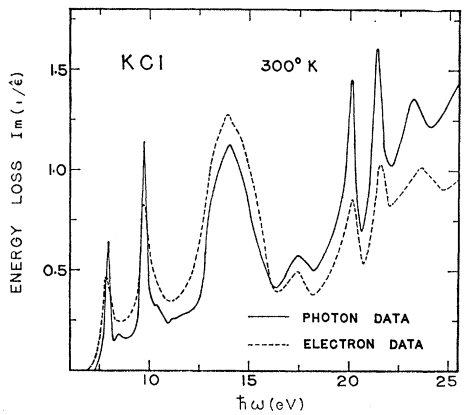

FIG. 11. The energy-loss function $\mathrm{Im}(1/\hat{\epsilon})$ for KCl, derived from a dispersion analysis of the optical-reflectance data of Fig. 2.

[29] M. Creuzburg, Z. Physik **196**, 433 (1966).
[30] F. Pradal, C. Gout, and B. Lahaye, Solid State Commun. 4, 119 (1966).
[31] J. C. Kelly and D. F. Lynch, Solid State Commun. **5**, 37 (1967).
[32] J. Geiger, P. Odelga, and H.-Chr. Pfeiffer, Phys. Status Solidi **15**, 531 (1966).
[33] P. E. Best, Proc. Phys. Soc. (London) **79**, 133 (1962).
[34] O. Sueoka, J. Phys. Soc. Japan **20**, 2226 (1965).
[35] S. L. Adler, Phys. Rev. **126**, 413 (1962).

TABLE I. Low-energy interband transitions in MgO, NaCl, and KCl, responsible for the analogous features in their optical spectra.

Band transition	Critical point	Observed energy (eV) MgO	NaCl	KCl
$\Gamma_{15} \rightarrow \Gamma_1$	M_0	7.77	8.97	8.69
$L_3 \rightarrow L_2'$	M_0	10.0	9.5	9.0
$\Lambda_3 \rightarrow \Lambda_1$	M_1	10.8	10.0	9.2
$X_5' \rightarrow X_1$	M_0	11.75	10.5	10.9
$\Delta_5 \rightarrow \Delta_1$	M_1	13.2	11.0	11.1
$\Sigma_4 \rightarrow \Sigma_1$	M_2	13.4	11.4	10.4
$X_5' \rightarrow X_3$	M_0	14.0	11.8	9.9
$L_3 \rightarrow L_3'$	M_0	15.7	12.9	11.2
$\Gamma_{15} \rightarrow \Gamma_{25}'$	M_0	16.0	13.2	11.6

respondence of spectral features below 18 eV, but also in the similarities of absolute magnitude. Creuzburg's data were obtained from transmission work on thin films and employed a 50-keV electron beam. The reasons for the appearance of structure beyond 18 eV in the optical data are not clear (some of the electron-loss data[30,34] do indicate weak structure, however). It is possible that the thin-film data are not entirely typical of the bulk material. On the other hand, the computed values of $\mathrm{Im}(1/\hat{\epsilon})$ are very sensitive to variations in ϵ_1 and ϵ_2 when the later are small, as is the case beyond 18 eV.

It is clear, by comparing Figs. 7 and 10, that most of the bands in the $\mathrm{Im}(1/\hat{\epsilon})$ spectrum correspond directly to features in ϵ_2, and are therefore due to one-electron excitations as described in Sec. 3 B. The dominant feature in Fig. 10 is the very strong band near 16 eV. This has a peak at 16.1 ± 0.1 eV in the photon data, and at 15.0 eV in the electron data. Other electron-loss data[30–34] variously estimated the peak to be at 15.5 eV or slightly above. Its asymmetry and strength are observed in all the reported electron energy-loss spectra. There is no corresponding feature in the ϵ_2 spectrum, and it is reasonable to assume that this energy loss is primarily due to many-electron or plasma excitation. For free electrons, the plasma frequency for resonance, ω_p, is given by

$$\omega_p^2 = 4\pi N e^2/m, \tag{4}$$

where N is the density of electrons participating in the collective excitation. Although the valence electrons cannot be considered as "free," application of Eq. (4), with $\omega_p = 16.1$ eV, yields a value of about 8 for the number of electrons per molecule participating in the excitation. Although most of the oscillator strength available for direct one-electron transitions from the valence band has been exhausted in the region below 15 eV (see preceding section), interband transitions are sufficiently close, energetically, to shift the plasma frequency from its free-electron value in any case.[36,37] Their presence probably explains much of the asymmetry and structure in the main resonance band.

In the case of KCl (Fig. 11), the agreement between the photon data and Creuzburg's electron-loss data[29] is extremely good in terms of spectral features. There is a discrepancy in the absolute intensity, however; the broken curve represents the electron data reduced by a factor of about 0.7. As in the case of NaCl, the majority of the peaks and shoulders in $\mathrm{Im}(1/\hat{\epsilon})$ are related to similar features in the ϵ_2 spectrum (Fig. 9), and result from direct interband transitions. The main peak in $\mathrm{Im}(1/\hat{\epsilon})$, lying at 14.1 ± 0.1 eV, has no counterpart in the ϵ_2 spectrum and should be interpreted as due to a plasma resonance. The peak occurs at 13.9 eV in Creuzburg's data, and at about the same energy in the other reports.[31–34,38] Use of Eq. (4), with $\omega_p = 14.1$ eV, gives a value of just under 9 for the number of "free electrons" per molecule. As in the case of NaCl, interband transitions are still too strong in this energy region (the ϵ_2 spectrum contains a strong peak at 12.5 eV) for much significance to be attached to this value, however.

4. SUMMARY

We have obtained the reflectance spectra of crystalline NaCl and KCl, and used a dispersion analysis to generate the ϵ_2 spectra. The similarities between these spectra (particularly that of NaCl) and that of MgO[10] suggested that an analysis of the spectra could be attempted on the basis of the band structure of MgO.[2,9] All of the prominent structure below 14 eV in the NaCl spectrum could be explained on this assumption. Extension to KCl was difficult until the marked lowering of the d-like conduction bands and the introduction of an exciton at X were taken into account. The prominent low-energy features were then identifiable as in the case of NaCl. We show the main transitions responsible for the strongest features of the low-energy spectra of MgO, NaCl, and KCl in Table I. It should be emphasized that the extent to which our analysis is correct is a measure of how well similar features in the experimentally observed spectra may be regarded as directly analogous to each other. There is a clear need for better resolution in the experimental data before more detailed identification can be made, particularly in the region beyond 12 eV. Some form of modulated reflectance technique may solve this problem, although there are several experimental difficulties in using such methods in the far ultraviolet.

[36] P. Nozieres and D. Pines, Phys. Rev. **113**, 1254 (1959).
[37] C. B. Wilson, Proc. Phys. Soc. (London) **76**, 481 (1960).
[38] M. Creuzburg and H. Raether, Solid State Commun. **2**, 354 (1964).